A&A 396, 157–169 (2002)
DOI: 10.1051/0004-6361:20021376

Astronomy & Astrophysics

Detectability and characteristics of the 2.223 MeV line emission from nearby X-ray binaries

N. Guessoum[1] and P. Jean[2]

[1] American University of Sharjah, College of Arts & Sciences, Physics Department, Sharjah, UAE
[2] Centre d'Etude Spatiale des Rayonnements, CNRS/UPS, 9 avenue du colonel Roche, 31028 Toulouse, France
e-mail: jean@cesr.fr

Received 31 July 2002 / Accepted 16 September 2002

Abstract. We present an application and an improvement of the model of Jean & Guessoum (2001) for the production of the 2.223 MeV line resulting from the capture of neutrons in the atmosphere of the secondary in an X-ray binary system. In this model, the neutrons are produced in the accretion disk around the compact primary star and radiated in all directions. The present treatment has fine-tuned and improved upon the previous model in several ways: (1) we have added CNONe nuclei in both the atmosphere of the secondary and the accretion disk around the compact object, making the production and interaction of the neutrons more realistic and accurate; (2) we have improved the physical modeling of the atmosphere of the secondary; and (3) we have considered the comptonization of the 2.223 MeV photons emitted and thus produced the spectrum of the emission both for the line and for the "continuum" below, down to some 100 keV of energy. We have performed a detailed investigation of the variation of the 2.223 MeV emissivity with respect to: the X-ray binary parameters (masses of the compact and secondary stars, separation, etc.), the rate and the model of accretion, and the metallicity of the accreted and atmospheric material. The mean fluxes, phasograms, and the spectra of the 2.223 MeV line have been calculated for several nearby X-ray binary sources, namely: A0620-00, XTE J1118+480, Cen X-4, GS 2000+25 and GRO J0422+32; and we have compared the results with present and future γ-ray spectrometer sensitivities (INTEGRAL's spectrometer SPI and the Compton Telescope).

Key words. X-rays: binaries – accretion, accretion disks – gamma-ray: theory – lines: profiles – nuclear reactions, nucleosynthesis, abundances

1. Introduction

Since the dawn of gamma-ray astrophysics, only a few decades ago, the line at 2.223 MeV, resulting from the capture of a neutron by a proton, has been recognized as one of the most interesting processes of this radiation domain, both from a theoretical and an observational viewpoint (e.g. Fichtel & Trombka 1981; Ramaty & Lingenfelter 1983). It has been considered in many astrophysical environments and conditions: solar flares, neutron-star surfaces, accretion disks around compact objects, etc. In each case, the characterization of the line has been shown to yield significant insights into the physics of the process and the environment.

First, the detailed spectroscopy of the line observed in solar flares was shown to constrain the physical models of the acceleration of ions as well as the physical parameters of the medium (e.g. Ramaty et al. 1995; Ramaty et al. 1996; Murphy et al. 1991; Share & Murphy 1995; Hua & Lingenfelter 1987; etc.). Secondly, Bildsten (1991) and Bildsten et al. (1993) showed that the line can help understand the acceleration of the protons and ambient material in the neutron-star's immediate environment as well as the channeling of the material onto the polar caps and the neutron capture by protons and iron nuclei there. Thirdly, Aharonian & Sunyaev (1984) considered the possibility of the 2.223 MeV emission in the accretion disks around black holes and showed that the copious production of neutrons by the hot inner part of the disk, followed by the capture of some of these neutrons by the ambient fast protons, would lead to such an emission, which could possibly be at detectable fluxes. Guessoum & Dermer (1988) considered a similar scenario with the neutrons produced in the accretion disk, but with some of them escaping it and reaching the secondary star companion, eventually undergoing capture (and other processes) in the atmosphere of the (relatively) cold companion, leading to the emission of a narrow line at 2.223 MeV. Jean & Guessoum (2001, hereafter referred to as JG, 2001) conducted a detailed investigation of this scenario, considering various accretion disk models and parameters, a range of compositions of

Send offprint requests to: N. Guessoum,
e-mail: nguessoum@aus.ac.ae

the accreted material and atmosphere of the secondary, and a host of processes suffered by the neutrons between their birth in the disk and their capture or decay in the atmosphere of the companion or in the space between the two objects in the binary system. JG (2001) showed that the 2.223 MeV line flux should be periodic due to the rotation of the binary system.

In all this time, however, and despite serious efforts to detect this emission from non-solar origins, no confirmed detection has been made, despite tantalizing announcements in the past (Jacobson 1978; McConnell et al. 1997). The most extensive searches for such an emission have been conducted using SMM (Solar Maximum Mission) data by Harris & Share (1991) and with COMPTEL (Compton Telescope instrument aboard the Compton Gamma-Ray Observatory) data by McConnell et al. (1997) and van Dijk (1996). The SMM survey was limited to essentially the galactic plane due to the nature of the mission itself; no emission was found there, and a 3-sigma upper limit of 1.0×10^{-4} photons $\mathrm{cm}^{-2}\,\mathrm{s}^{-1}$ was set on the steady emission from the Galactic center and from Sco X-1. Similarly, upper limits of $\sim 1\text{–}2 \times 10^{-4}$ photons $\mathrm{cm}^{-2}\,\mathrm{s}^{-1}$ were set on the Cyg X-1 and Cyg X-3 point sources (averaged steady emission). The more recent all-sky survey at 2.223 MeV conducted by McConnell et al. (1997) found few features in the sky and showed, as expected, no diffuse emission at this energy through both maximum-entropy and maximum-likelihood algorithms. One spot stood out, however, at $(l, b) = (300°, -30°)$, with $\sim 3.7\sigma$ significance, although it did not correspond to any X-ray binary that could be linked to this emission by way of the neutron production and capture scenario mentioned previously. The only counterpart that could possibly be linked to this emission feature was the white dwarf RE J01317-053, whereby a flare-like strongly magnetic stochastic acceleration of protons could lead to a substantial production and capture of neutrons in the atmosphere of the white dwarf. (Efforts to investigate and model this emission are ongoing.) As to the search for possible emission from X-ray binary systems such as interests us here, McConnell et al. (1997) considered the van Paradijs (1995) catalog of sources but found no evidence of emission at 2.223 MeV; 3-sigma flux limits were typically set in the range of $1\text{–}2 \times 10^{-5}$ photons $\mathrm{cm}^{-2}\,\mathrm{s}^{-1}$ for such sources as Cyg X-3, Sco X-1, 4U 1916-05, 4U 1616-67, and 4U 1820-30. And lastly, van Dijk (1996) compiled a list of upper-limit 2.223 MeV binary-source radiation fluxes based on COMPTEL observations of 27 black-hole candidates. These upper limits range from 1 to 5×10^{-5} photons $\mathrm{cm}^{-2}\,\mathrm{s}^{-1}$.

In anticipation of INTEGRAL's (INTErnational Gamma-Ray Laboratory) search for emission at this (and other) energy(ies), and following up on our general model for 2.223 MeV line emission in X-ray binary systems (JG 2001), we have conducted a theoretical investigation of specific sources that we selected for their potential detectability parameters, namely their short distance from earth, but also other factors that we will delineate in the main sections of this paper. We have retained the main features of our model, namely: accretion of matter from the secondary star onto the compact object by way of a hot accretion disk around the primary star, production of neutrons via a network of nuclear reactions; escape of the neutrons from the gravitational well due to their sufficiently high energies (10 MeV or more); arrival of a fraction of them at the atmosphere of the secondary star; propagation, slow-down, thermalization, re-escape from and sometimes return to the atmosphere; and, finally, capture by hydrogen nuclei, leading to the production of the gamma-ray photons, which will then escape (after some possible comptonization). We have, however, fine-tuned and improved upon the model in several ways: we have added CNONe nuclei in both the atmosphere of the secondary and the accretion disk around the compact object (this makes the production and interaction of the neutrons more realistic and accurate); we have improved the physical modeling of the atmosphere of the secondary; and we have finally considered the comptonization of the 2.223 MeV photons emitted, and we thus produced the spectrum of the emission both for the line and for the "continuum" below, down to some 100 keV of energy.

The general scenario and model thus remains the same as in JG (2001). We have, however limited our set of parameters for the accretion disk models. In our previous work we considered five such models: ADAF (Advection-Dominated Accretion Flows); ADIOS (Advection-Dominated Inflow-Outflow Solutions); SLE (Shapiro-Lightman-Eardley two-temperature disk model); and GK (Guessoum & Kazanas neutron-viscosity, uniform temperature model) with the ion temperature set at either 10 MeV or 30 MeV. In each case we varied some of the basic parameters, such as the viscosity parameter α (either 0.1 or 0.3), the accretion rate $\dot{M}$ (ranging from 10^{-11} to 10^{-8} solar masses per year); the composition of the disk (90% H & 10% He or 10% H & 90% He), the electron temperature, the inclination of the system with respect to the observer (earth), etc. Since we have already studied the variation of the emission flux with these parameters for a generic X-ray binary source, we will limit ourselves in this work to only a small subset of parameters (e.g. $\dot{M} = 10^{-9}\ M_{\odot}$/yr, $\alpha = 0.1$) for each of the 4 models (ADAF, ADIOS, SLE, GK) previously considered; we will, however, discuss the consequences of a variation of these parameters on the flux of the emission in specific cases, should such variations have important implications with regard to the detectability of the radiation.

This paper is structured as follows: in Sect. 2, we present a concise update on our neutron production and capture model, particularly the inclusion of CNONe elements in the accreted matter and in the secondary star's atmosphere as well as the consequences of these additions, and also the improvements made on the secondary star's atmospheric model and other changes made compared to our previous treatment; in Sect. 3, we present the set of nearby X-ray binary sources selected in this study, including the selection criteria and the physical characteristics of the sources (masses of the primary and secondary stars, separation, composition of the atmosphere and accretion disk, rotation periods, etc.); in Sect. 4, we present the results of our study, particularly the expected fluxes of 2.223 MeV emission, the phasograms, and the predicted spectra for each source, and we discuss the relevance of these results in view of INTEGRAL's capabilities as well as future high-sensitivity instruments (e.g. the high-resolution Compton Telescopes, as proposed by Boggs & Jean 2001); we conclude in Sect. 5 with prospects for this study and subsequent ones.

2. Neutron production and capture model (Update)

As mentioned above, the general features of our neutron production and capture model remain mostly unchanged. In particular, the accretion disk models are essentially the same as those used in JG (2001), and the processes of propagation, slow-down, thermalization, escape, and capture of the neutrons in the atmosphere of the secondary star have not been modified in any important way. Matter is accreted at a given rate $\dot{M}$ and with a given elemental composition; it then gets heated to a temperature $T_{\rm i}$ that depends on r (the distance from the compact object) according to the specific accretion disk model used; the nuclei thus undergo a series or network of nuclear reactions, the most important ones being those that produce neutrons (from the break up of ^{4}He or CNONe). The neutrons then scatter rather freely in the medium, since they are not confined by the magnetic field, and so they fly out isotropically from the point where they were produced. Those that have a kinetic energy larger than the local gravitational binding (potential) energy will escape, provided their directions are "outward"; the rest of the neutrons and the other nuclei continue to be swept inward by the flow and get swallowed by the compact object. This process is described by two intertwined parts of our numerical program: a) the accretion disk model (ADAF, ADIOS, SLE, or GK) equations for $T_{\rm i}$, ρ, $v_{\rm r}$, etc. given in JG (2001); b) the nuclear reaction rates and abundance variations, which are calculated by a set of differential equations for each species.

The only new addition to this part of the scenario is the inclusion of CNONe nuclei in the accretion flow; this implies the addition of a series of new nuclear reactions (and differential equations), leading to the destruction and production of various elements and species, and – of prime interest to us – of neutrons.

The main neutron-producing nuclear reactions that have been added are:

$$\begin{aligned}
&\mathrm{p}+^{12}\mathrm{C} \longrightarrow \mathrm{n} + X\\
&\alpha+^{12}\mathrm{C} \longrightarrow \mathrm{n} + X\\
&\mathrm{p}+^{14}\mathrm{N} \longrightarrow \mathrm{n} + X\\
&\alpha+^{14}\mathrm{N} \longrightarrow \mathrm{n} + X\\
&\mathrm{p}+^{16}\mathrm{O} \longrightarrow \mathrm{n} + X\\
&\alpha+^{16}\mathrm{O} \longrightarrow \mathrm{n} + X\\
&\mathrm{p}+^{20}\mathrm{Ne} \longrightarrow \mathrm{n} + X\\
&\alpha+^{20}\mathrm{Ne} \longrightarrow \mathrm{n} + X
\end{aligned}$$

for which the cross sections were taken from the compilation of Hua et al. (2002). It is interesting to note that these reactions have lower threshold energies and higher cross section values (by factors ranging from 2 to 10) than the corresponding reactions that involve H and He (i.e. in a pure hydrogen-helium plasma, as in our previous work). This will translate into higher neutron rates and therefore higher 2.223 MeV photon fluxes in some cases (depending on the composition of the material).

The main element-destroying nuclear reactions that have been added are:

$$\begin{aligned}
&\mathrm{p}+^{12}\mathrm{C} \longrightarrow ^{11}\mathrm{B}/^{11}\mathrm{C} + \mathrm{p} + \mathrm{p/n}\\
&\alpha+^{12}\mathrm{C} \longrightarrow ^{11}\mathrm{B}/^{11}\mathrm{C} + \alpha + \mathrm{p/n}\\
&\mathrm{p}+^{14}\mathrm{N} \longrightarrow ^{11}\mathrm{C} + \alpha\\
&\alpha+^{14}\mathrm{N} \longrightarrow ^{11}\mathrm{C}/^{11}\mathrm{B}/^{10}\mathrm{B} + \alpha + ^{3}\mathrm{H}/^{3}\mathrm{He}/^{4}\mathrm{He}\\
&\alpha+^{14}\mathrm{N} \longrightarrow ^{6}\mathrm{Li} + 3\alpha\\
&\mathrm{p}+^{16}\mathrm{O} \longrightarrow ^{11}\mathrm{B}/^{11}\mathrm{C} + \alpha + 2\mathrm{p}/^{2}\mathrm{H}\\
&\alpha+^{16}\mathrm{O} \longrightarrow ^{11}\mathrm{B}/^{11}\mathrm{C} + 2\alpha + \mathrm{p/n}\\
&\mathrm{p}+^{20}\mathrm{Ne} \longrightarrow X + Y\\
&\alpha+^{20}\mathrm{Ne} \longrightarrow X + Y.
\end{aligned}$$

For the first seven reactions, cross-section data were taken from Ramaty et al.'s (1997) compilation; for the last two reactions, no data were found, so cross sections were assumed to equal those of the similar reactions that involve ^{16}O.

Production of neutrons is then computed for any given initial composition of the accreted material for each specific accretion disk model and parameters (α, $\dot{M}$, etc.). The mass of the compact object, which enters the calculation, is taken to be either 1 $M_\odot$ in the "generic" case or the specific value for the primary of the system under consideration. Escape fractions, calculated in exactly the same way as in JG (2001), that is to say precisely the same way as in Guessoum & Kazanas (1990), then allow us to obtain the rates of neutrons leaving the disk isotropically, and from the solid angle subtended by the companion star (using the radius of the secondary and the separation between the primary and the secondary) the rates of neutrons impinging into the atmosphere of the companion star are determined. The spectrum of neutrons escaping the accretion disk is assumed to be a Maxwellian distribution with a temperature of $kT = 10$ MeV, truncated at 5 MeV because the gravitationnal potential of the primary compact object retains the neutrons of lower energy.

In the atmosphere, the same scenario occurs as in our previous work. Some of the neutrons get thermalized; some are captured by nuclei, others decay or escape the secondary, if after several scatterings their kinetic energies become larger than the gravitational potential energy binding them to the star. Two improvements have been made to this part of the work: a) the CNONe nuclei have been included here too, and they do participate in the above processes (thermalization, scattering, nuclear reactions, which may lead to a change in the abundances of some elements/isotopes, possibly observable – as we shall discuss later); b) the modeling of the atmosphere of the secondary star has been substantially improved, by taking into account the density and temperature variation as a function of the depth. Indeed, in JG (2001) the atmospheric model consisted of a uniform density and temperature material even though these physical conditions are known to increase gradually with the depth. This can significantly affect the efficiency of neutron capture in low-density and extended atmospheres. In such cases, the timescale for neutrons to thermalize can be larger than their half-life, resulting in a reduction of the neutron capture rate.

The temperature and density profile of main-sequence low-mass stars have been roughly modeled using the

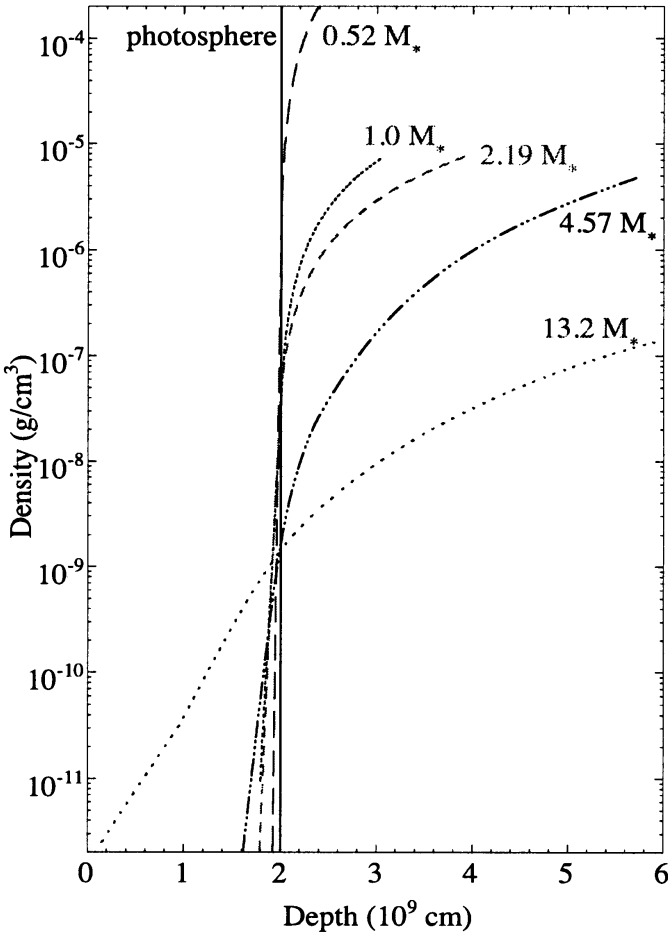

Fig. 1. Density profile models of secondary star atmospheres.

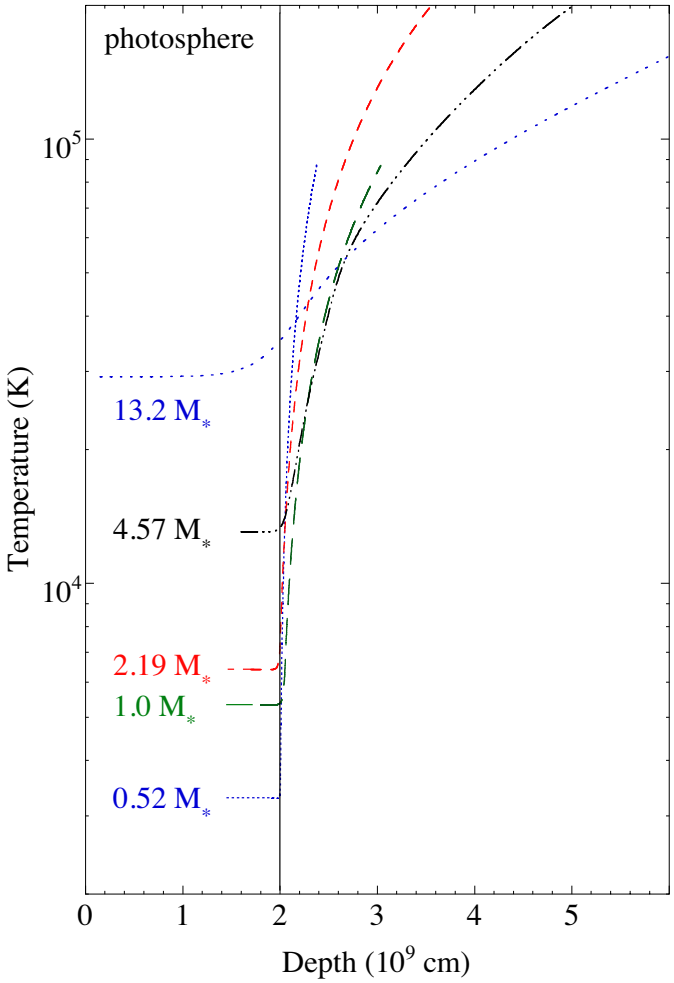

Fig. 2. Temperature profile models of secondary star atmospheres.

LTE atmosphere calculation method described in Mihalas (1970), which consists of solving the hydrostatic equilibrium equation in the photospheric region starting with a grey temperature stratification. In the convective region the temperature and density are calculated by considering an adiabatic process. The atmosphere of high-mass stars (e.g. the secondary of Cyg X-1) are modeled using the Tlusty code of Hubeny & Lanz (1997). It has been assumed that the accretion does not substantially modify the structure of the atmosphere.

Figures 1 and 2 present a plot of the density and the temperature variation with the depth in the atmosphere of the secondary for five cases of secondary main sequence stars: M_s = 0.52, 1.0, 2.19, 4.57 and 13.2 $M_\odot$. The stellar parameters (radius, effective temperature) used to model the atmosphere of these stars have been taken from Gray (1992), which explains why these specific values of M_s have been adopted here.

Ultimately the neutrons either get captured (mostly by H and ^{3}He nuclei, but also by other isotopes, such as ^{12}C, ^{14}N and ^{16}O) or decay (in the atmosphere or in the outer space where they would have escaped). Our propagation program, updated from the old GEANT/GCALOR extensive simulation code that we used and described in JG (2001), then computes the number of 2.223 MeV photons thus produced as well as the energy and direction of emission of each. This allows us to determine the rate/emissivity of the radiation as well as its spectrum (line and continuum due to the comptonization of the emitted photons) and phasogram (variation with the phase/rotation of the system with respect to the observer).

We have thus undertaken two kinds of calculations:

- a) General calculations of the fluxes, spectra, and phasograms for a "generic" source where some of the physical characteristics are given "standard" values (M_{co} = 1 $M_\odot$, M_s = 1 $M_\odot$, a solar composition of the atmosphere and the accretion disk, a separation of $a = 3\,R_\odot$ between the primary and the secondary) and then one parameter (such as $\dot{M}$) is made to vary. This exploration of the parameter space is useful in that it will allow us (and others) in the future to determine the flux of the 2.223 MeV radiation for any source provided its characteristics are known, without specifically needing to rerun our program. These results are also useful to understand the effect of the different physical parameters (e.g. abundance, mass of the secondary...) on the 2.223 MeV emissivity.
- b) Specific-source calculations for the systems chosen and described in the following section, where we select a number of promising candidates for INTEGRAL's (and future instruments') exploration of the sky at this energy.

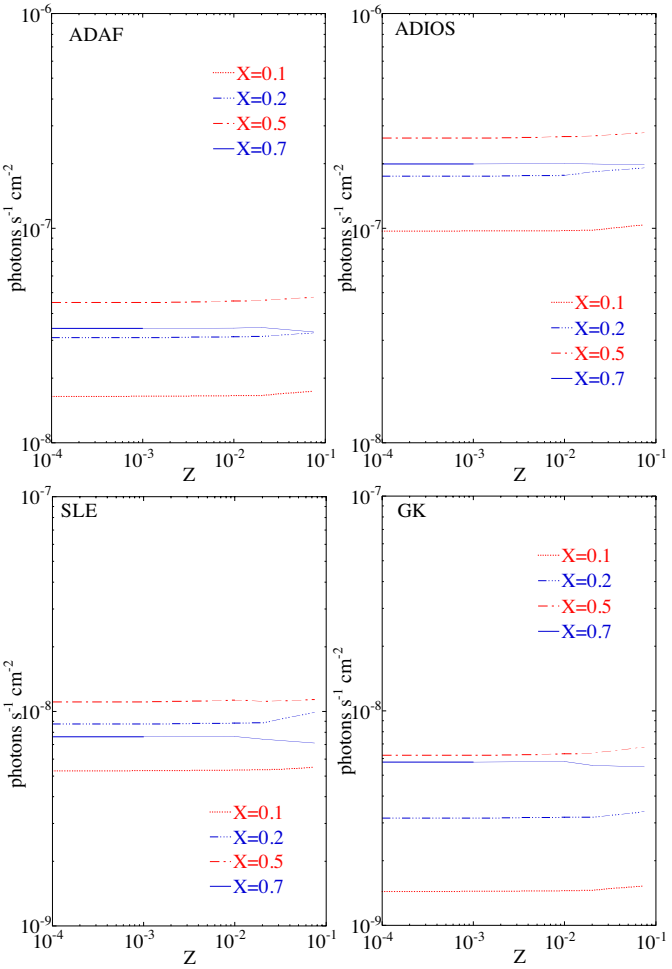

Fig. 3. Flux of the 2.223 MeV line as a function of the metallicity, for several abundances of H. The accretion disk models ADAF, ADIOS, SLE and GK are presented separately.

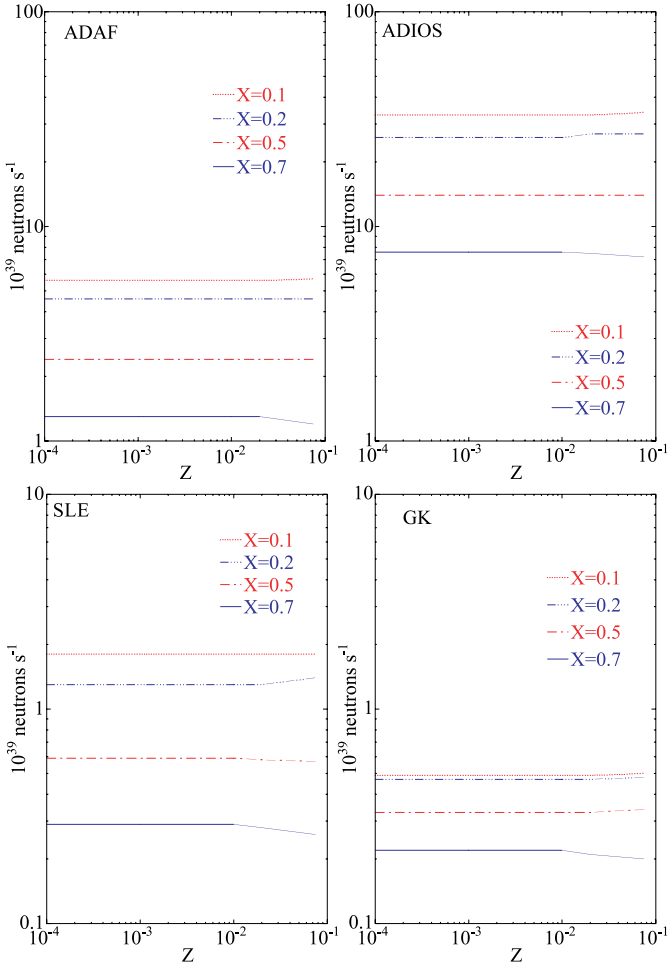

Fig. 4. Rate of neutrons produced in the accretion disk as a function of the metallicity, for several abundances of H. The accretion disk models ADAF, ADIOS, SLE and GK are presented separately.

Before we present our selected sources and the results of our calculations for those, we deem it appropriate to present the general results for the "generic" runs first. These results show how the mean 2.223 MeV line flux varies with the abundance, the type of the secondary star, the accretion disk model, and the separation of the binary system.

Figure 3 shows the mean flux of 2.223 MeV emission, $F_{2.2}$, as a function of the CNONe total abundance Z, with X (the fraction, by mass, of H) given values ranging from 0.1 to 0.7; and Y (the fraction, by mass, of He) being related to X and Z through $X + Y + Z = 1$. Note that in all our cases the relative abundances of C, N, O, Ne (among themselves) is always the same as in the solar case: 32.3% of C, 6.7% of N, 53.5% of O, and 7.6% of Ne (Cameron 1981), all other heavy elements being neglected in the accretion model. Several accretion disk models are presented separately with $\dot{M} = 10^{-9}\ M_\odot$/yr. In the ADAF and ADIOS models, the viscosity parameter $\alpha = 0.1$. All other parameters are given the "standard" values ($M = 1\ M_\odot$, $\dot{M} = 10^{-9}\ M_\odot$/yr, $M_s = 1\ M_\odot$, $a = 3\ R_\odot$, etc.). All fluxes in this sections are computed for a "standard" distance of 1 kpc between the source and the earth and an inclination of the binary system of 0°.

The 2.223 MeV flux does not vary significantly with the metallicity. In order to understand the variation of the 2.223 MeV flux with Z (Fig. 3) we must recall that abundances influence not only the neutron rate from the accretion disk but also the efficiency of the secondary atmosphere in producing 2.223 MeV photons.

The yield of neutron in the accretion disk as a function of the metallicity is shown in Fig. 4. The first observation one readily makes is that for any given value of X (and thus Y), the neutron production depends only slightly on Z, and then only for relatively high Z. This is easily understood when one recalls that Z is the abundance of CNONe *by mass*, which means that by number these nuclei represent but a very small fraction of all the plasma particles; indeed for every proton, one finds only 10^{-3} "heavy" nuclei for solar composition. Clearly these are not going to contribute any significant new quantities of neutrons. When the value of Z becomes appreciable (~0.1), we notice that the neutron production increases (slightly) for low values of X but decreases for higher values of X. This is explained by the changes in the helium abundance Y, as this quantity is the essential factor determining the final yield in neutrons. Increasing X implies decreasing Y for a given value of Z, but when X and Z become too high the neutrons obtained

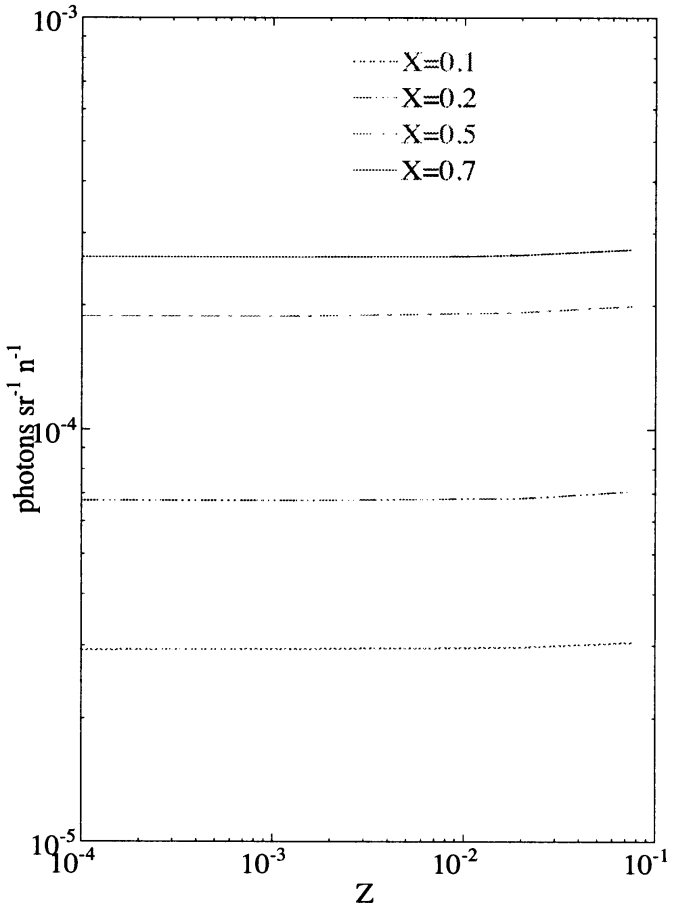

Fig. 5. 2.223 MeV line emissivity of the atmosphere as a function of the metallicity for several abundances of H.

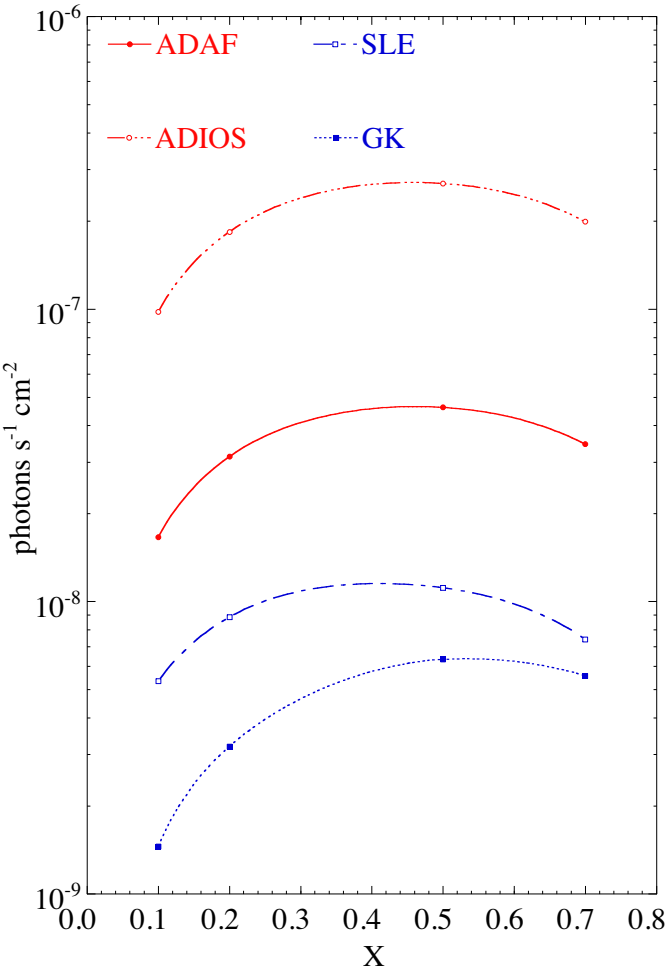

Fig. 6. Flux of the 2.223 MeV line as a function of H abundance. The accretion disk models ADAF, ADIOS, SLE and GK are presented separately.

from the breakup of CNONe do not compensate for the loss due to the reduction in the helium abundance.

Figure 5 shows the emissivity of 2.223 MeV as a function of Z. The emissivity is proportional to the efficiency of the secondary atmosphere to capture neutrons (and to allow the escape of 2.223 MeV photons) for a constant neutron rate. This emissivity increases slightly at high Z values because for a given X, an increase in Z implies a decrease of the abundance of He (Y) and therefore a decrease in the neutron capture rate by ^{3}He, which is competing with the n-capture by H.

Figure 6 shows the 2.223 MeV flux as a function of X for a solar metallicity ($Z = 0.02$). This figure shows clearly the contribution of both the production of neutrons in the accretion disk and the atmospheric response. Indeed, the neutron yield in the accretion disk increases with decreasing values of X (i.e. increasing abundance of He), since neutrons are mostly produced by the breakup of He (Fig. 4). On the other hand, the efficiency of the atmosphere in producing 2.223 MeV photons (i.e. n-capture by H) increases with increasing value of X (Fig. 5), neutrons being preferentially captured by ^{3}He at low X. We then logically obtain a maximum of the 2.223 MeV flux around $X \approx 0.5$.

Figure 7 presents the mean 2.223 MeV line flux as a function of the accretion rate $\dot{M}$ for the ADAF and ADIOS accretion model and two values of the viscosity parameter, all other parameters given the "standard" values. The graph confirms that the neutron production is roughly proportional to the square of both $\dot{m}$ and α^{-1}, especially at low values, as the density of the plasma n is proportional to $\dot{m}/\alpha$. At higher values of $\dot{M}$, however, the neutron production saturates – and so the curves tend to flatten somewhat – as the helium (source for neutrons) becomes scarce.

Figure 8 is similar to the previous one but with M_s being varied and all other parameters given the "standard" values except that the binary system separation a is adapted for each secondary mass value, such that the solid angle between the neutron source and the secondary star stays constant (i.e. identical to the case $M_s = 1\ M_\odot$, $R_s = 1\ R_\odot$ and $a = 3\ R_\odot$), simply to avoid solid angle variation of the 2.223 MeV line flux.

Two reasons will explain why the flux decreases when the secondary mass increases. The first and foremost effect is the reduction of gravity in the atmosphere, which induces (a) a reduction of the density and an increase of its height extension (see Fig. 1), so that the neutrons take more time to thermalize and thus decay more frequently than get captured by H; (b) an increase in the fraction of neutrons that escape the atmosphere. The second effect is due to the increase of the separation when

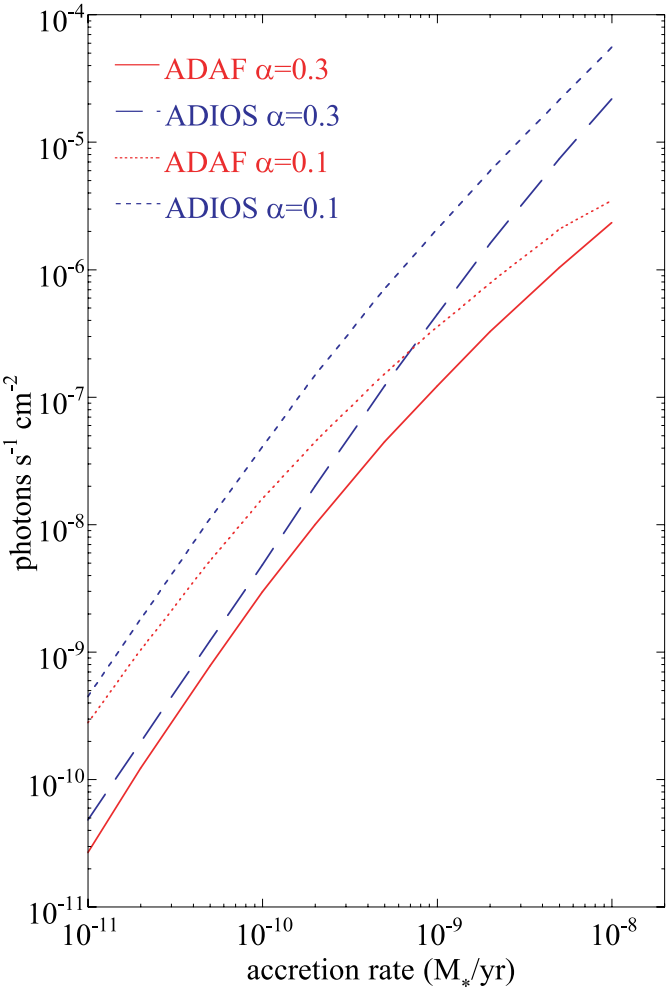

Fig. 7. Flux of the 2.223 MeV line for a "generic" source (M_{co} = 1$_\odot$, M_s = 1 $M_\odot$, solar abundances, a = 3 $R_\odot$, d = 1 kpc) as a function of the accretion rate for the disk models ADAF and ADIOS and two values ofthe viscosity parameter α.

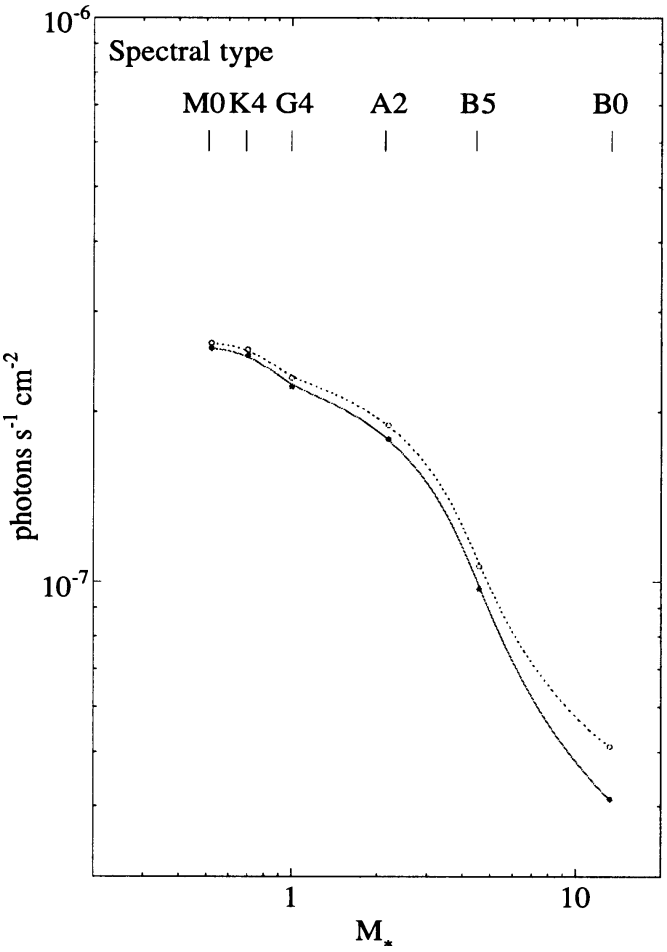

Fig. 8. Flux of the 2.223 MeV line as a function of the secondary mass. The dotted line shows the variation of the flux assuming that the neutrons do not decay in flight between the accretion disk and the secondary star's atmosphere.

the secondary's mass increases. Indeed, as the solid angle between the accretion disk and the secondary star is constant, the flux of neutrons reaching the atmosphere decreases with increasing a due to the enhancement of the fraction of neutrons decaying in flight. This fraction is 2% for 0.52 $M_\odot$ ($a \approx 1.8\ R_\odot$) and ≈20% for 13.2 $M_\odot$ ($a \approx 20\ R_\odot$). In order to bring out the effect of the secondary mass parameter on the 2.223 MeV line flux, a second curve (dotted line) is plotted in Fig. 8, where the decay of neutrons in flight between the disk and the atmosphere is "turned off"; this shows the atmospheric response with a constant impinging neutron flux. This figure therefore shows that the characteristic of the secondary (mass, radius and consequently the density profile of its atmosphere) has an important effect on its efficiency to produce the 2.223 MeV line, independently of the separation, the metallicity, and the accretion rate.

The loss of neutrons due to their decay in flight between the accretion disk and the secondary is clearly visible in Fig. 9, which shows the 2.223 MeV line flux as a function of a (the separation between the two stars), all other parameters given the "standard" values. For comparison, the dotted curve shows the variation of the flux assuming it depends only on the solid angle subtended by the secondary star, which is proportional to the neutron flux impinging on the atmosphere. However, results presented in Fig. 9 for separations greater than 6 $R_\odot$ are not physically representative of accreting XRB's since the secondary star does not then fill its Roche lobe if the mass of the compact object is lower than 20 $M_\odot$.

A fraction of the produced 2.223 MeV photons are comptonized by electrons in the secondary atmosphere. Some of the scattered photons escape the secondary and constitute a continuum emission below 2.223 MeV. This emission has been modeled using the GEANT code, and the results are presented in Fig. 10. The continuum level logically follows the flux of the 2.223 MeV line. The intensity of the Compton component is roughly a factor 100 below the continuum sensitivity of present γ-ray telescopes; for instance, the continuum sensitivity of SPI and IBIS instruments of the INTEGRAL mission are $\approx 4 \times 10^{-4}$ photons s^{-1} cm^{-2} MeV^{-1} and 2×10^{-4} photons s^{-1} cm^{-2} MeV^{-1} respectively in the 100 keV–1 MeV energy range.

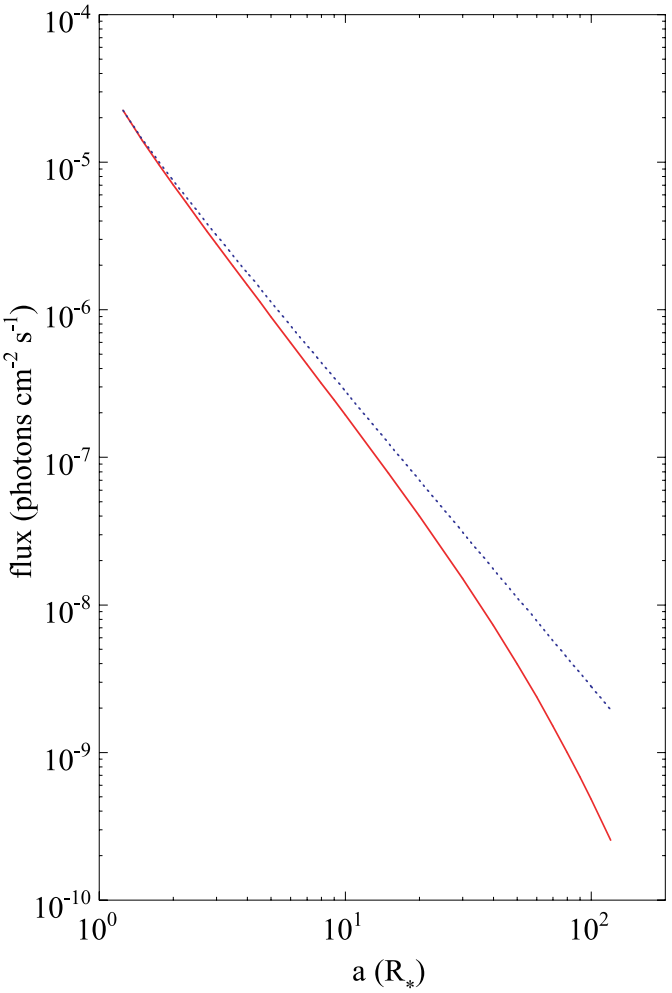

Fig. 9. Flux of the 2.223 MeV line as a function of the binary system separation. The dotted curve shows the variation of the flux due only to the change in the solid angle between the accretion disk and the secondary.

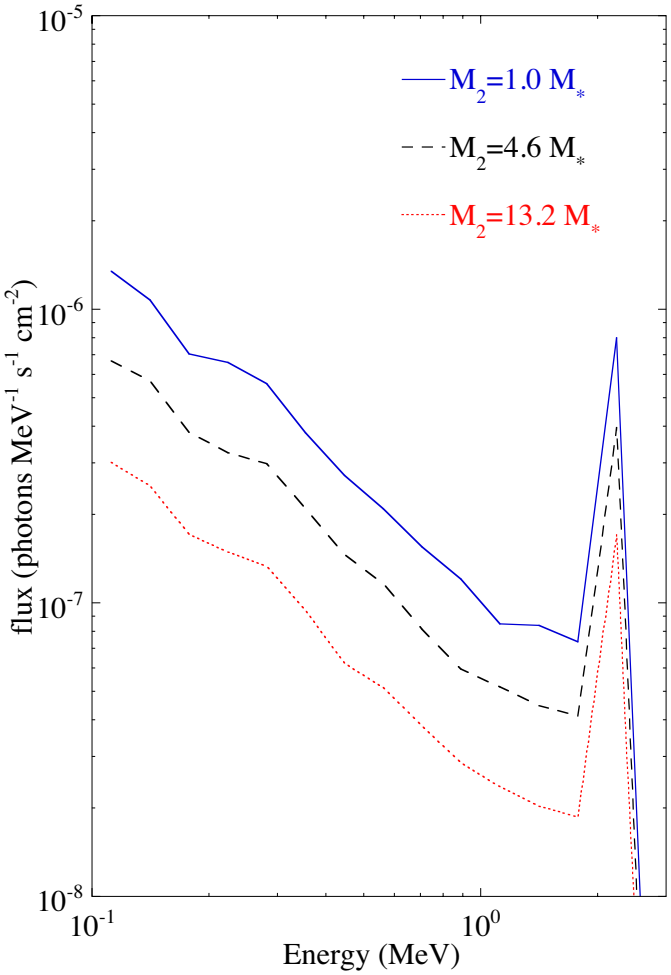

Fig. 10. Continuum hard X-ray spectrum as a function of the secondary mass. The accretion rate is 10^{-9} $M_\odot$ yr^{-1} (ADIOS), and the separation of the binary system is 3 $R_\odot$.

3. The nearby X-ray binaries of interest

With potential INTEGRAL detection of the radiation in mind, we have considered only nearby sources, i.e. those that are at distances less than about 2.5 kpc. Furthermore, for the 2.223 MeV emission flux to be reasonably high (higher than 10^{-6} photons cm^{-2} s^{-1}, roughly) we have limited our interests to binaries with short separations, which can be inferred indirectly from the orbital periods; we have tended to reject sources with orbital periods P greater than about 5 days. But in order to carry out our calculations fairly accurately, we needed as much information about each source as possible: distance from earth, orbital period or separation, inclination of the system with respect to the observer's line of sight, the masses of the compact object and of the secondary star, the accretion rate (from X-ray luminosities in normal or, preferably, in burst states), and the secondary's atmospheric temperature (from the spectral type). As the composition is not precisely determined, for these sources we have used a standard solar composition.

We have been able to obtain such complete, though not always very accurate, information for 5 sources, which we present in Table 1 under the title "fairly well-known sources" or "most promising sources".

Our best candidates, all physical parameters considered, are: A0620-00 (also known as V616 Mon) and XTE J1118+480 (also known as V* KV UMa), mostly due to their short distances to earth and to the closeness of the secondary to the compact object in each case. We shall discuss this in more detail in the following section after the results of flux calculations are presented.

For another dozen sources, we have either found only partial or contradictory information, particularly about their distances to earth (sometimes a source was listed as having a distance of 0.5 to 7.0 kpc, sometimes no value was found in the literature). These sources have been grouped in Table 2, titled "less fully known sources" or "less promising sources"; they might be checked in future observational surveys or searches through INTEGRAL or future instruments.

4. Results and discussion

For each of our Table 1 sources we have calculated the mean fluxes $F_{2.2}$, the phasograms, and the spectra, for a limited set of accretion disk models and free parameters (α, $\dot{M}$, etc.).

Table 1. Most promising and fairly well kwown XRB sources and their parameters, used to calculate the 2.223 MeV flux. These have been obtained from: (1) Gelino et al. (2001); (2) McClintock et al. (2001); (3) Haswell et al. (2002); (4) Chevalier et al. (1989); (5) Menou & McClintock (2001); (6) Callanan et al. (1996); (7) Beekman et al. (1996); (8) Filipenko et al. (1995); (9) Webb et al. (2000).

Source	d (kpc)	i (deg)	a ($R_\odot$)	M_{co} ($M_\odot$)	M_s ($M_\odot$)	R_2 ($R_\odot$)	T_{eff} (K)	Ref.
A0620-00	1.16	41	4.5	11	0.7	0.7	4600	(1)
XTE J1118+480	1.8	70	2.5	7.2	0.6	0.7	4130	(2), (3)
Cen X-4	1.2	40	3.5	1.4	0.15	0.65	4300	(4), (5)
GS 2000+25	2	65	4.5	10	0.5	0.7	4500	(6), (7)
GRO J0422+32	1.4	48	2.35	3.6	0.4	0.55	3900	(8), (9)

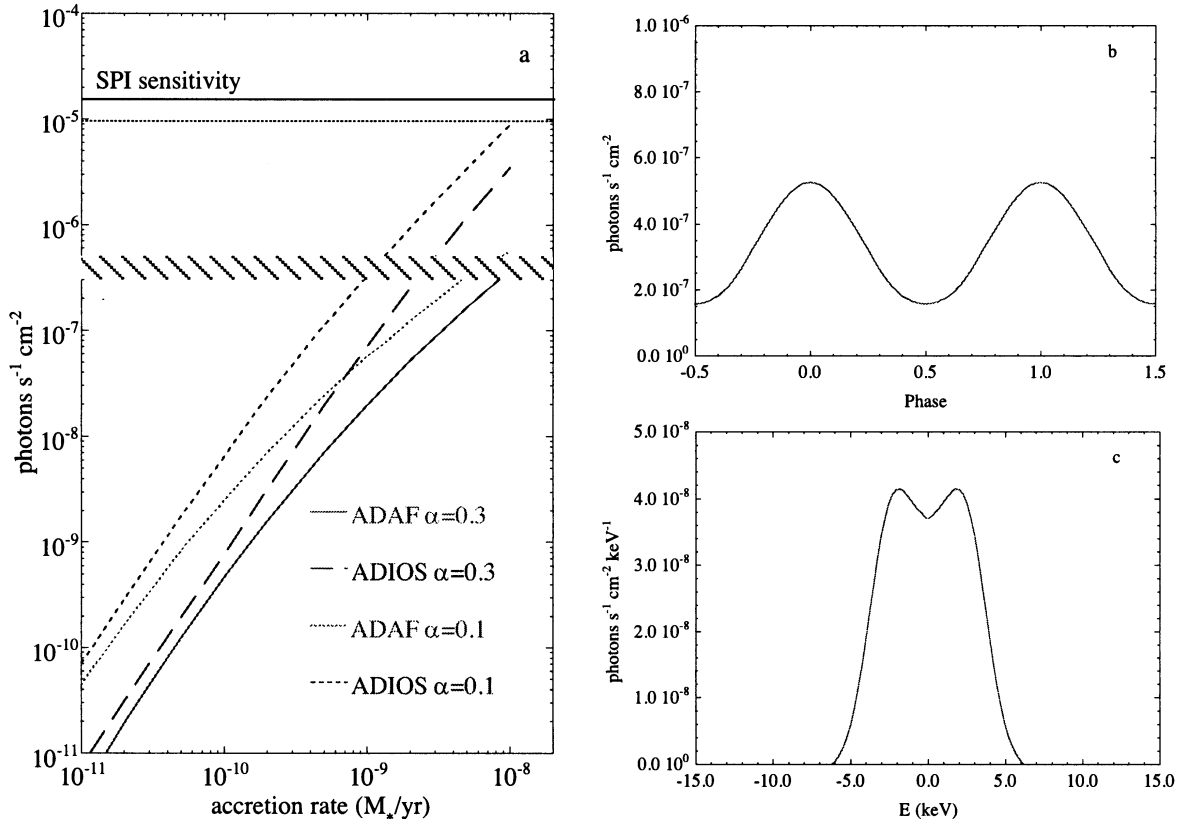

Fig. 11. Results for A0620-00: **a)** mean 2.223 MeV flux calculated as a function of the accretion rate and model. The horizontal solid and dotted lines show the SPI normal and improved sensitivity (3σ, 10^6 s of observation), the stripped zone represents the sensitivity range of the next generation high-resolution Compton Telescope. **b)** Phasogram of the 2.223 MeV flux estimated with an ADIOS model (α = 0.1) for an accretion rate of 10^{-9} $M_\odot$ yr^{-1}. **c)** Line shape for the same accretion conditions as in **b)**. The line shape shown has been convoluted with the spectral resolution of SPI (≈3 keV).

The following Figs. 11a–c to 15a–c present our results. Figures 11a to 15a also show the limit of INTEGRAL's SPI (spectrometer) expected 3σ flux sensitivity (solid horizontal line), taking into account the line width, as well as an "improved" sensitivity line (dotted horizontal line) where we have devised a scheme whereby the regular recording and binning of photons over many complete phase cycles allows for an improvement of the statistics with respect to the instrumental background. Indeed, firstly we can improve the signal-to-noise ratio when recording photons only during the fraction (≈50% depending on the shape of the phasogram) of the binary period when the emission flux is significant. Secondly, since the signal-to-noise ratio of narrow lines is better than the one for broad lines, we can improve the sensitivity by processing the data, applying an energy shift correction to each detected photon and thus build a narrow gamma-ray line. These methods can be performed only if we know the orbital parameters of the binary systems, which allow us to calculate the spectral shift and the phasogram of the gamma-ray line as a function of time. In these conditions we can reduce the observation time for a 3σ detection with SPI by factor 2 to 3 depending on the shape of the line and the amplitude of the phasogram.

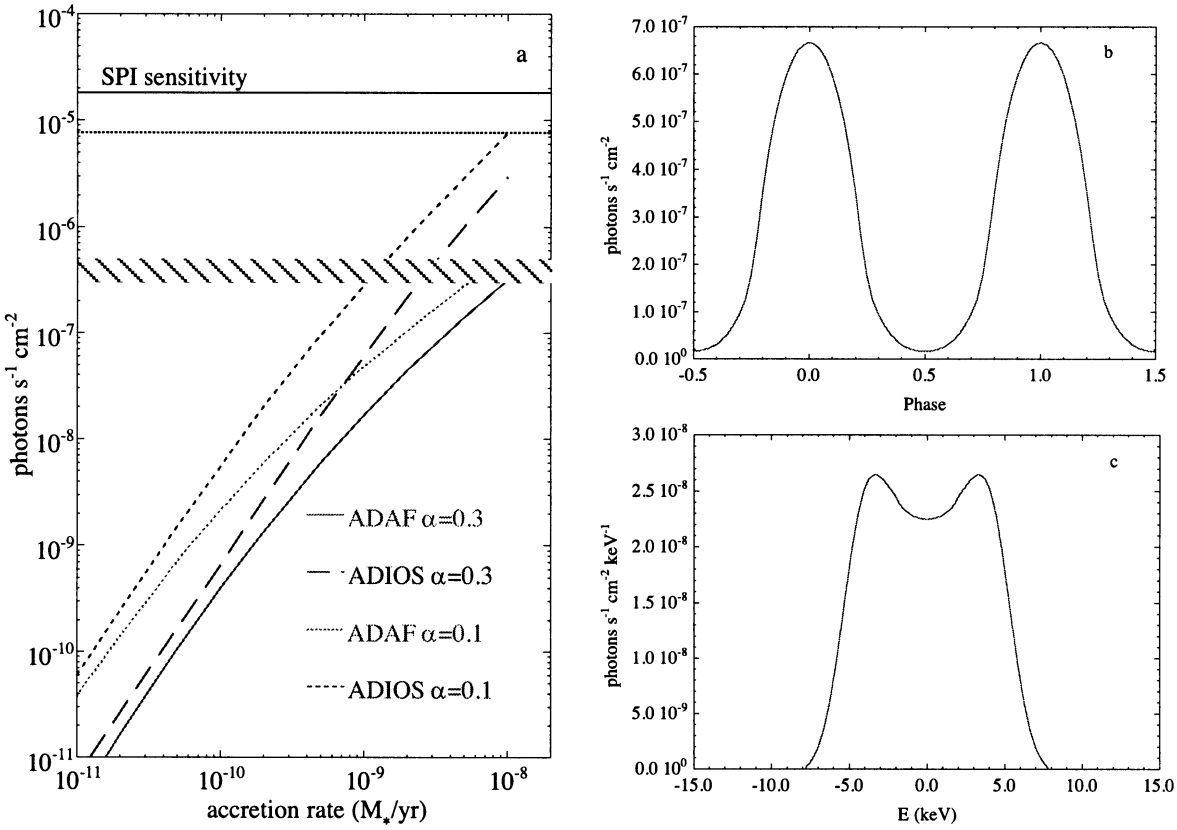

Fig. 12. Same as Fig. 11 but for XTE J1118+480.

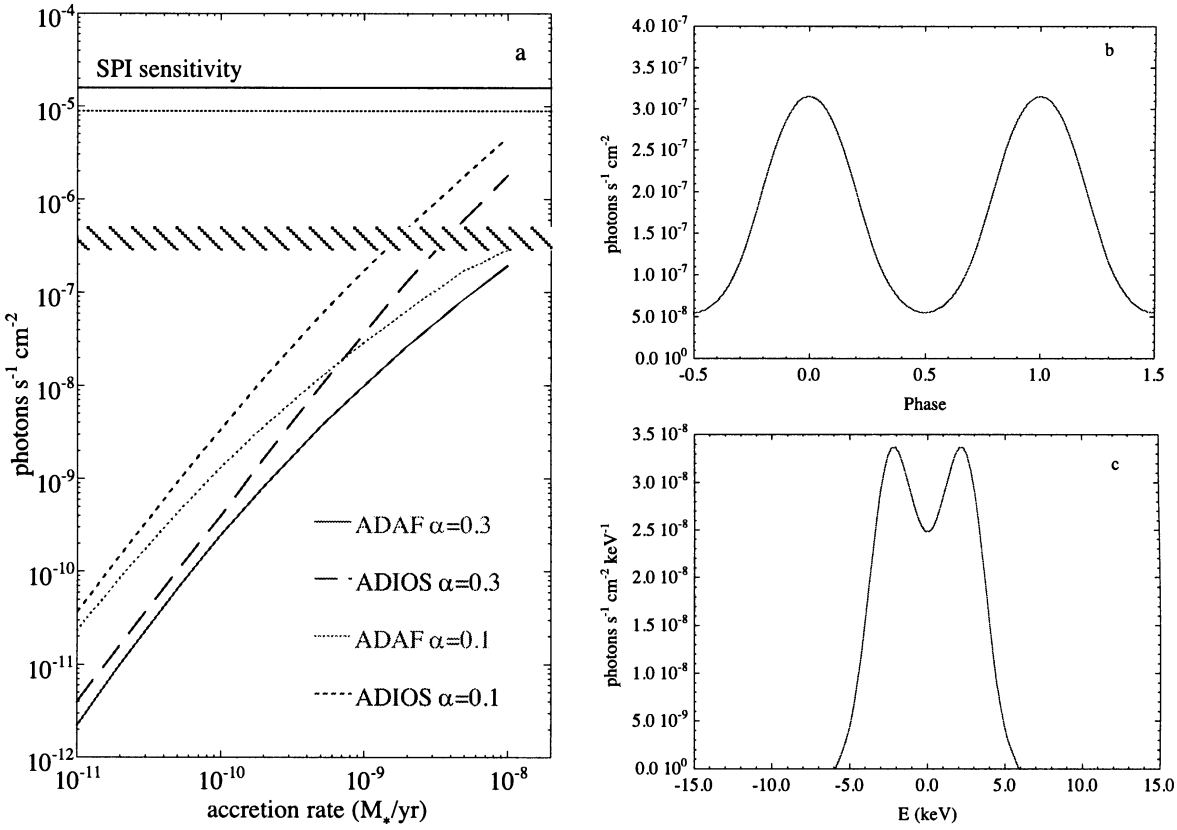

Fig. 13. Same as Fig. 11 but for GRO J0422+32.

Table 2. Less promising or less fully known X-ray binary candidates for the 2.223 MeV line emission. Distance and type have been obtained from: (1) Herrero et al. (1995); (2) Barziv et al. (2001); (3) Sadakane et al. (1985); (4) Heinz & Nowak (2001); (5) Mason & Cordova (1982); (6) Herczeg & Maloney (1999); (7) Pavlenko et al. (1996); (8) Shahbaz et al. (1997); (9) Chevalier & Ilovaisky (1998); (10) Reig et al. (1996); (11) Haberl & Sasaki (2000); (12) Negueruela (1998); (13) Steeghs & Casares (2002); (14) Macomb & Gehrels (1999).

name	d (kpc)	Period (days)	Type	Ref.
Cyg X-1	2.5	5.6	HMXRB	(1)
Vela X-1	1.9	8.96	HMXRB	(2), (3)
X1822-371	2	?	LMXRB	(4), (5)
GS 2023+34	2.3	6.48	LMXRB	(6), (7), (8)
GRS 1124-684	3–4	0.43	LMXRB	(8), (14)
V662 Cas	1.4–7	11.6	HMXRB	(9), (10)
V635 Cas	4	24.3	HMXRB	(11)
V0332+43	3	34.3	HMXRB	(11)
RX J0146+6121	2.3	large	HMXRB	(11), (12)
V725 Tau	0.33–2	111	HMXRB	(9), (12)
V801 Cen	0.3–3.1	187	HMXRB	(9), (12)
Sco X-1	0.7–1.3	0.232	LMXRB	(13)
GRO J1719-24	2.5	?	LMXRB	(14)
GRO J1655-40	3.2	2.62	LMXRB	(14)
N Oph 1977	6	0.52	LMXRB	(14)

The improvement in sensitivity with this method increases with increasing XRB inclination, since the latter tends to increase the variation of the flux and thus lower the mean value, and the phase-binning can help by picking up the higher values only. Since most of the mean 2.223 MeV line fluxes of XRB candidates are below the detection threshold of SPI, we also show in Figs. 11a to 15a the calculated/estimated range in sensitivity of the next generation of high-resolution gamma-ray instruments, e.g. the Compton Telescope (Boggs & Jean 2001) for the same observing time as SPI ($\approx$10 days).

It is clear from the figures that the detection of a 2.223 MeV emission from these sources by INTEGRAL is not going to be a straightforward matter. For many of these the probability of such detection is indeed very small, even in the best parameter-value conditions. However, for A0620-00 and XTE J1118+480, the detection is possible, though only for the highest accretion rate in the ADIOS model with $\alpha = 0.3$. In any case, this investigation will serve as a guide and reference for observers and theorists both in the INTEGRAL era and beyond (with the current planning for more advanced, future detectors). Even in the case of "negative results" (upper limits for specific sources), the above figures will help constrain the physical parameters of these systems, particularly with regard to the accretion models and their parameters.

There is one last effect that we wish to emphasize here, especially since it too could become an interesting issue for both observers and theorists in the future. This concerns the enhancement of abundances of LiBeB elements in the atmosphere of the secondary star through the breakup of a fraction of the CNONe nuclei by the bombarding neutrons. This effect has already been pointed out and investigated by Guessoum & Kazanas (1999), who proposed this scenario and treated a "generic" case of it. It was also recalled in JG (2001). But now with our fuller, more systematic treatment of a much wider parameter space for the binary systems, and indeed with our treatment of specific X-ray sources with their own physical characteristics we are in a position to determine more specifically how much enhancement there would occur in each case (which isotopes, how much, etc.). In fact our neutron propagation and capture code GEANT/GCALOR can readily compute "final" abundances for a large variety of isotopes, although one must still add the processes of convection, which will mix the material and contribute to the destruction of some elements, most particularly lithium, and stellar wind, which will eject some of the produced material into the interstellar medium.

This lithium enhancement in such sources is already becoming an interesting problem, since at least three of the "prime" X-ray binary sources from our Table 1 have been shown to have significantly enhanced lithium abundances: A0620-00, Cen X-4 (Martin et al. 1992, 1994, 1996), and GS 2000+25 (Filippenko et al. 1995; Harlaftis et al. 1996). On the other hand, Harlaftis et al. (1997) did not detect any abnormal lithium abundances in Nova Ophiuchus 1977 (V* V2107 Oph), which is in our Table 2. These two facts (detection of Li enhancement in three sources of our "prime" list and absence of abnormal abundance of Li in the only source that has been observed from our "Grade B" list) seem to suggest some relation between the two effects (emission of 2.223 MeV radiation and Li enhancement). We plan to investigate this issue in a future work.

5. Conclusions

We have conducted a systematic investigation of the 2.223 MeV line emission from nearby X-ray binary sources under the assumption of neutrons being produced in the accretion disk and flying out to bombard the atmosphere of the secondary, where they would be captured to produce the signature gamma-ray line. In this work we have followed up and improved upon our model (Jean & Guessoum 2001) by, on the one hand, adding CNONe nuclei both in the accretion disk and the atmosphere of the secondary star, and on the other hand modeling the atmosphere more realistically.

We have thus produced fluxes of the radiation of interest in "generic"/"standard" cases, but more importantly, we have applied the model to a number of sources selected specifically for their potential detectability by INTEGRAL. For those, we obtained fluxes, phasograms, and spectra of both the line and its continuum (from the comptonization of some of the line photons). We have compared our results with the capabilities of SPI, INTEGRAL's spectrometer, and we also pointed out a way to take advantage of the variation of the flux with the phase of the binary source in order to maximize and even improve upon the nominal detection limits of the instrument in such cases. We have further looked down the road for prospects of detections with future, high-resolution instruments.

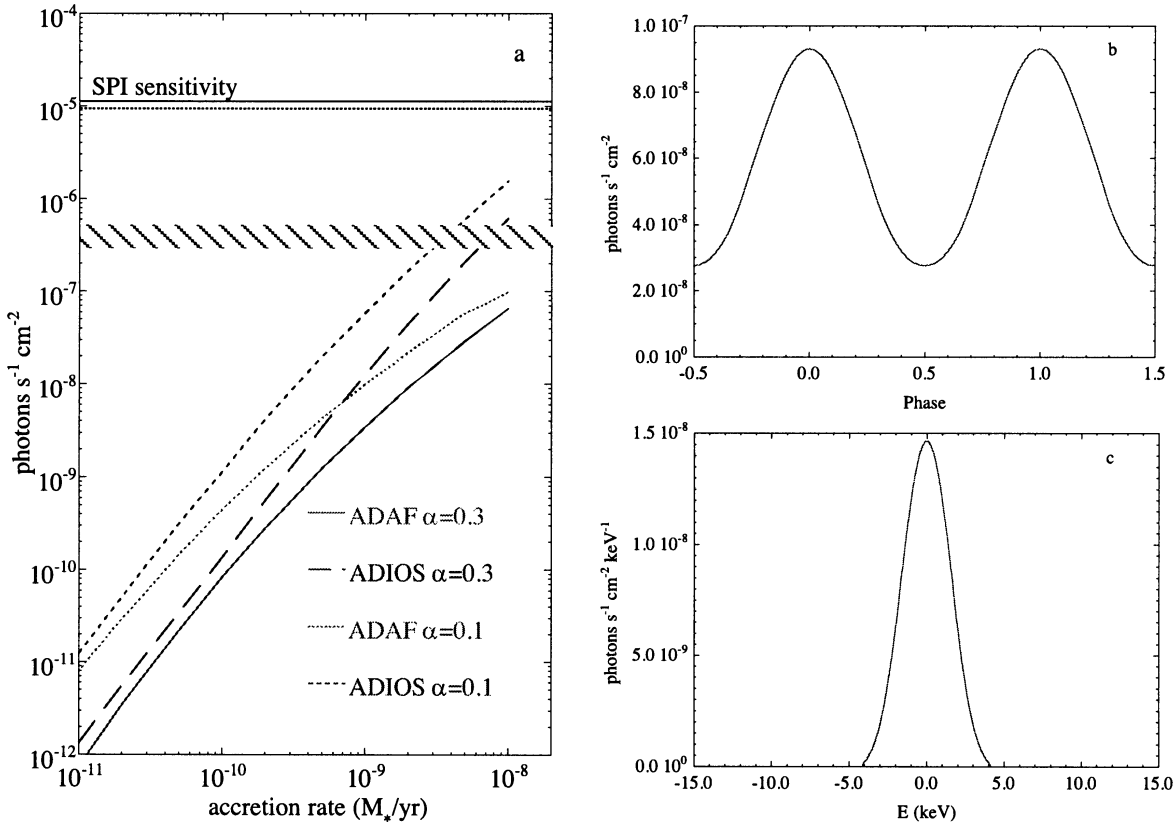

Fig. 14. Same as Fig. 11 but for Cen X-4.

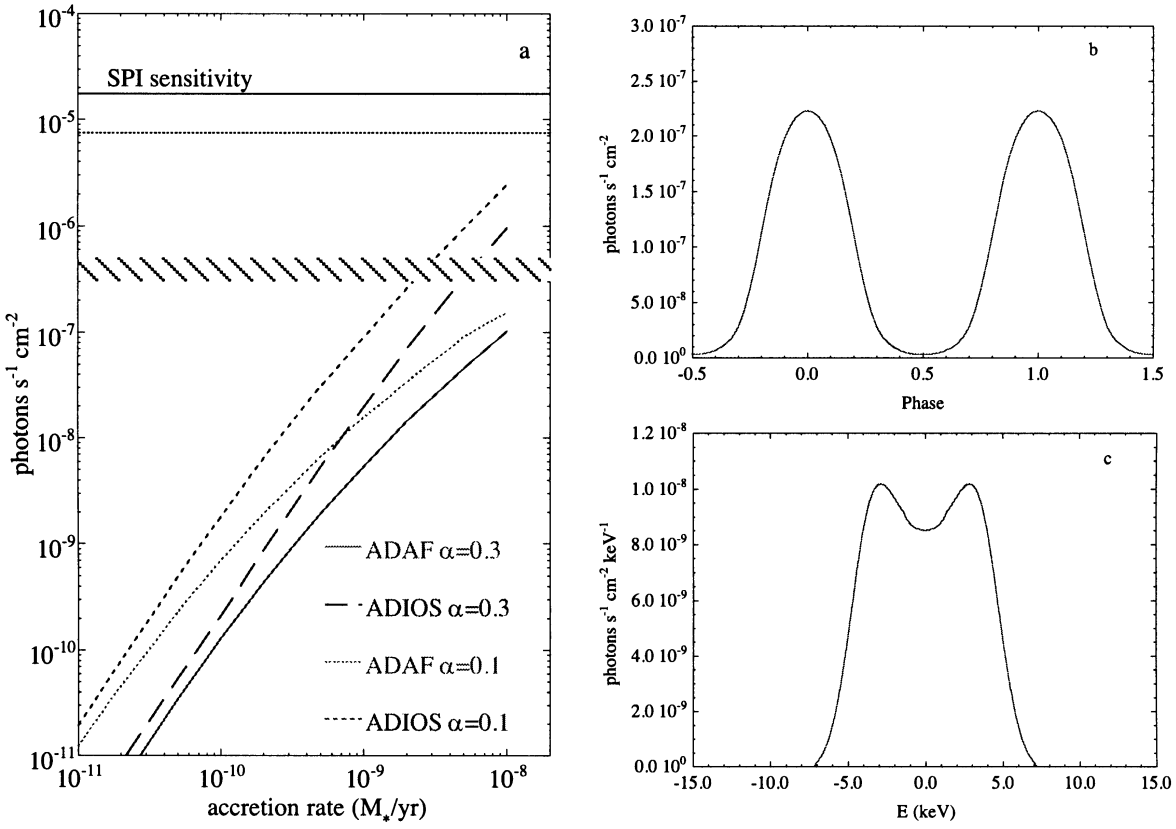

Fig. 15. Same as Fig. 11 but for Ginga 2000+25.

Finally we noted with interest the prospect of lithium (and other isotopes) enhancement in the secondary star's atmosphere by neutron spallation of CNONe elements, an effect that has already been observed for 3 of our "prime" candidates of 2.223 MeV detection and has already previously been interpreted as the result of neutron bombardment of the secondary (Guessoum & Kazanas 1999). We will turn our attention to this issue in a near-future treatment.

We wish to emphasize here that an INTEGRAL search for this emission from the candidate sources we listed in Table 1 (our "Grade A" sources), and even those listed in Table 2 (our "Grade B" sources), will yield interesting consequences whether the detections are positive or negative. Indeed any measurement or upper limit will place constraints on the physical conditions of these systems, particularly with regard to the accretion disk models governing them. Looking further into the future, this treatment and the lists of candidates presented herein, should encourage those who are already planning and designing future high-sensitivity gamma-ray instruments and missions to keep a strong interest in the 2.223 MeV line from XRB sources.

Acknowledgements. We thank V. Tatischeff for his useful suggestions. N. Guessoum would like to acknowledge the support of the American University of Sharjah (UAE) as well as the Centre d'Étude Spatiale des Rayonnements (Toulouse, France), where much of this work was conducted. He also wishes to thank Prs. P. von Ballmoos and J. P. Roques for the facilities provided at the CESR.

References

Aharonian, F. A., & Sunyaev, R. A. 1984, MNRAS, 210, 257
Barziv, O., Kaper, L., van Kerkwijk, M. H., Telting, J. H., & van Paradijs, J. 2001, A&A, 377, 925
Boggs, S. E., & Jean, P. 2001, A&A, 366, 1126B
Beekman, G., Shahbaz, T., Naylor, T., & Charles, P. A. 1996, MNRAS, 281, L1
Bildsten, L. 1991, in Gamma-Ray Line Astrophysics, AIP Conf. Proc. 232, ed. P. Durouchoux, & N. Prantzos (New York: AIP), 401, 615
Bildsten, L., Salpeter, E. E. & Wasserman, I. 1993, ApJ, 408, 615
Callanan, P. J., Garcia, M. R., Filippenko, A. V., McLean, I., & Teplitz, H. 1996, ApJ, 470, L57
Cameron, A. G. W. 1981, Essays in Nuclear Astrophysics (Cambridge Univ. Press)
Chevalier, C., Ilovaisky, S. A., van Paradijs, J., Perdersen, H., & van der Klis, M. 1989, A&A, 210, 114
Chevalier, C., & Ilovaisky, S. A. 1998, A&A, 330, 201
Fichtel, C. E., & Trombka, J. I. 1981, Gamma-Ray Astrophysics, NASA SP-453
Filippenko, A. V., Matheson, T., & Barth, A. J. 1995, ApJ, 455, 139
Filippenko, A. V., Matheson, T., & Ho, L. C. 1995, ApJ, 455, 614
Gelino, D. M., Harrison, T. E., & Orosz, J. A. 2001, AJ, 122, 2668
Gray, D. F. 1992, The observation and analysis of stellar photosphere, 2nd ed. (Cambridge University press), 430
Guessoum, N., & Dermer, C. D. 1988, in Nuclear Spectroscopy of Astrophysical Sources, ed. N. Gehrels, & G. H. Share (New York: AIP), AIP Conf. Proc., 107, 332
Guessoum, N., & Kazanas, D. 1990, ApJ, 358, 525
Guessoum, N., & Kazanas, D. 1999, ApJ, 512, 332
Haberl, F., & Sasaki, M. 2000, A&A, 359, 573
Harlaftis, E. T., Horne, K., & Filippenko, A. V. 1996, PASP, 108, 762
Harlaftis, E. T., Steeghs, D., Horne, K., & Filippenko, A. V. 1997, AJ, 114, 1170
Harris, M. J., & Share, G. H. 1991, ApJ, 381, 439
Haswell, C. A., Hynes, R. I., King, A. R., & Schenker, K. 2002, MNRAS, 332, 928
Heinz, S., & Nowak, M. A. 2001, MNRAS, 320, 249
Herrero, A., Kudritzki, R. P., Gabler, R., Vilchez, J. M., & Gabler, A. 1995, A&A, 297, 556
Herczeg, T. J., & Maloney, M. T. 1999, JAAVSO, 27, 22
Hubeny, I., & Lanz, T. 1997 `http://tlusty.gsfc.nasa.gov/`
Hua, X. M., & Lingenfelter, R. E. 1987, ApJ, 323, 779
Hua, X. M., Kozlovsky, B., Lingenfelter, R. E., Ramaty, R., & Stupp, A. 2002, ApJS, 140, 563
Jacobson, A. S., et al. 1978, Gamma-Ray Spectroscopy in Astrophysics (NASA T.M. 79619), 228
Jean, P., & Guessoum, N. 2001, A&A, 378, 509, (JG 2001)
Macomb, D. J., & Gehrels, N. 1999, ApJS, 120, 325
McClintock, J. E., Garcia, M. R., Caldwell, N., et al. 2001, ApJ, 551, L147
McConnell, M., Fletcher, S., Bennett, K., et al. 1997, in Proc. of the Fourth Compton Symp., ed. C. D. Dermer, M. S. Strickman, & J. D. Kurfess (New York: AIP), AIP Conf. Proc. 410, 1099
Martin, E. L., Rebolo, R., Casares, J., & Charles, P. A. 1992, Nature, 358, 129
Martin, E. L., Rebolo, R., Casares, J., & Charles P. A. 1994, ApJ, 435, 791
Martin, E. L., Casares, J., Molaro, P., Rebolo, R., & Charles, P. 1996, New Astron., 1, 197
Mason, K. O., & Cordova, F. A. 1982, ApJ, 262, 253
Menou, K., & McClintock, J. E. 2001, ApJ, 557, 304
Mihalas, D. 1978, Stellar Atmospheres, 2nd ed. (Freeman, San Francisco)
Murphy, R. J., Ramaty, R., Reames, D. V., & Kozlovsky, B. 1991, ApJ, 371, 793
Negueruela, I. 1998, A&A, 338, 505
Pavlenko, E. P., Martin, A. C., Casares, J., Charles, P. A., & Ketsaris, N. A. 1996, MNRAS, 281, 1094
Ramaty, R., & Lingenfelter, R. E. 1983, Adv. Space Res., 3, 123
Ramaty, R., Mandzhavidze, N., Kozlovsky, B., & Murphy, R. J. 1995, ApJ, 455, L193
Ramaty, R., Mandzhavidze, N., & Kozlovzky, B. 1996, in High Energy Solar Physics, ed. R. Ramaty, N. Mandzhavidze, & X. M. Hua (New York: AIP), AIP Conf. Proc. 374, 172
Reig, P., Chakrabarty, D., Coe, M. J., et al. 1996, A&A, 311, 879
Sadakane, K., Hirata, R., Jugaku, J., et al. 1985, ApJ, 288, 284
Shahbaz, T., Naylor, T., & Charles, P. A. 1997, MNRAS, 285, 607
Share, G. H., & Murphy, R. J. 1995, ApJ, 452, 933
Steeghs, D., & Casares, J. 2002, ApJ, 568, 273
van Dijk, R. 1996, Ph.D. Thesis, 148
van Paradijs, J. 1995, X-ray Binaries, ed. W. H. G. Lewin, J. van Paradijs, & E. P. J. van den Heuvel (Cambridge University press)
Webb, N., Naylor, T., Ioannou, Z., Charles, P. A., & Shahbaz, T. 2000, MNRAS, 317, 528